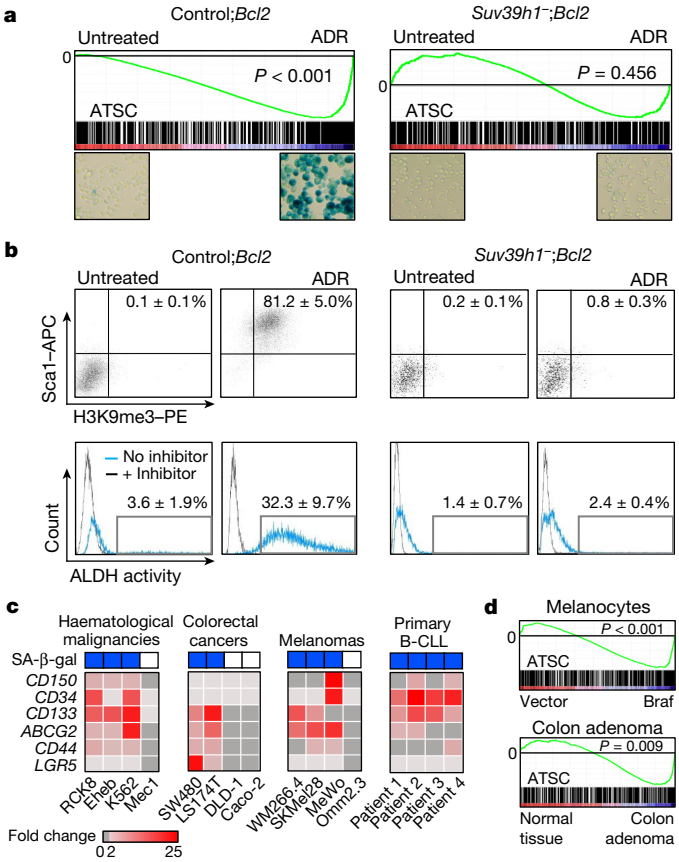

Figure 1 | Therapy-induced senescent cancer cells acquire phenotypic and functional stemness features. a, GSEA of an adult tissue stem cell profile[17] (ATSC; top) in matched pairs of ADR-exposed versus untreated control;*Bcl2* lymphomas ($n = 12$; left) and *Suv39h1*$^{-}$;*Bcl2* lymphomas ($n = 5$; right). TIS lymphomas display more than 80% SA-β-gal-positive blue cells[9] (representative photomicrographs from four independent experiments). **b**, Co-expression of the stem cell marker Sca1 and the TIS marker H3K9me3 (top) in lymphoma cells as in **a**, and aldehyde dehydrogenase (ALDH) activity with and without the ALDH inhibitor diethylaminobenzaldehyde (bottom) by flow cytometry. Mean percentage of positive cells ± s.d.; $n = 5$ biologically independent samples each. **c**, Expression of the indicated stem-cell-related genes in various human cancer cell lines or primary B-CLL samples by quantitative PCR (qPCR), related to their ability to enter TIS (ADR-senescent, blue; non-senescent despite ADR exposure, white (see Extended Data Fig. 1c for details)). Colours reflect fold induction (between ADR-treated and untreated samples) from one representative out of three independent experiments (cell lines) or four individual samples from patients with B-CLL. Transcripts below the detection level are shown in light grey. **d**, GSEA of the adult tissue stem-cell profile in the publicly available transcriptome of *BRAF*^{V600E}-infected melanocytes, which senesce in response to Braf activation[7,28] (left; seven matched pairs), and colon adenomas, which are known to contain a large proportion of senescent cells[29] (right; five *Apc*$^{Min/+}$ mouse adenoma biopsies and six healthy colon tissue samples).

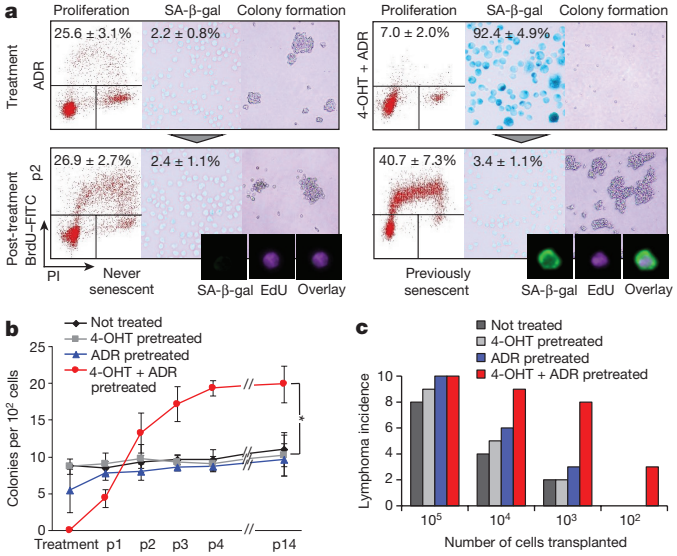

Figure 2 | Senescence-released (previously senescent) lymphomas display higher tumour-initiating capacity than their never senescent counterparts. a, Growth properties of conditionally senescent *Suv39h1*$^{-}$;*Bcl2*;*Suv39h1*-ER^{T2} lymphoma cells after five days of ADR ± 4-OHT treatment (treatment), and subsequent passages in 4-OHT/ADR-free medium (post-treatment, p1–p2; each passage reflecting seven days in culture) presented as proliferation (left, mean BrdU/PI-marked S-phase fraction ± s.d., $n = 5$ biologically independent samples; BrdU, 5-bromo-2′-deoxyuridine; PI, propidium iodide), SA-β-gal staining (middle, mean positive cells ± s.d., $n = 5$ biologically independent samples), and colony formation (right, quantified in **b**). Flow microscopy images (bottom) of the fluorescent SA-β-gal mark together with the proliferation marker EdU (passage 1 shown, see Extended Data Fig. 2g for details) demonstrates the outgrowth of senescent (SA-β-gal^{+}) cells. Representative photomicrographs from four independent experiments. **b**, Colony counts of lymphoma cells (treated as in **a**) in extended serial passaging (p1–p14). Graphs show mean colony numbers ± s.d., $n = 3$ individual lymphomas. Two-tailed unpaired *t*-test with Welch's correction, comparing ADR- and 4-OHT+ADR pretreated cells at p14. $^{*}P < 0.05$. **c**, Tumour initiation after transplantation of different numbers of *Suv39h1*$^{-}$;*Bcl2*;*Suv39h1*-ER^{T2} lymphoma cells pre-exposed to the indicated treatments *in vitro*. Bars reflect numbers of lymphoma-bearing mice out of 10 animals per group transplanted, within an observation period of up to 100 days. $P < 0.001$ for comparing never senescent and previously senescent groups (χ^2).

cells, presented with increased aldehyde dehydrogenase (ALDH) and ATP-binding cassette (ABC) transporter activities (Fig. 1b, bottom, and Extended Data Fig. 1d), both typical properties of stem cells. When assessing human malignancies of various origins, we found a notable upregulation of stem-cell-related transcripts selectively in TIS-capable cell lines as well as samples from patients with primary B-cell chronic leukaemia (B-CLL) (Fig. 1c and Extended Data Fig. 1c, e, f). Moreover, the acquisition of stemness-related properties can also be found in the process of oncogene-induced and replicative senescence in cells of various tissue types, including melanocytes, colon mucosa and breast epithelial cells (Fig. 1d and Extended Data Fig. 1g). Hence, cancer cells of mouse and human origin acquire novel stem-cell features upon entering cellular senescence.

To test whether senescence-associated stemness (SAS) translates into different tumour behaviour upon release from the division block, we generated switchable model systems (using 4-hydroxytamoxifen (4-OHT)-inducible essential senescence mediators Suv39h1 or p53) that can enter full-featured senescence with increased levels of stem-cell-related transcripts and proteins only when exposed to both 4-OHT and ADR (Fig. 2a and Extended Data Fig. 2a–c). After changing to ADR- and 4-OHT-free medium to switch Suv39h1 or p53 off again, single-cell analyses revealed that senescent cells resumed sustainable proliferation within a few days; that is, they became first double-positive for the retained fluorescence-based senescence marker (a vital stain) and 5-ethynyl-2′-deoxyuridine (EdU) incorporation, indicating restarted DNA synthesis (with the proliferation-repressive H3K9me3 mark gradually vanishing), before SA-β-gal activity was eventually lost and S-phase activity fully regained (Fig. 2a and Extended Data Fig. 2d–g). Therefore senescence is, in principle, a reversible condition, which becomes evident when essential senescence maintenance genes are no longer expressed. Importantly, serial replatings in colony-formation experiments of such previously senescent cells led to significantly more colonies compared to the aliquot of never senescent cells